SLAC National Accelerator Lab
LCLS-II TN-18-05
August 2018

Soft X-ray Self-Seeding at LCLS-II

Moving the infrastructure from the U8 to the U10 SXR undulator girder location

G. Marcus*, E. Hemsing, A. Lutman
SLAC, Menlo Park, CA 94025

Abstract

The SXRSS infrastructure will nominally be installed in the U8 girder location in the LCLS-II SXR undualtor line in the baseline scenario. This technical note details the physics justifications for moving the installation downstream two undulator sections to the U10 girder location.

*gmarcus@slac.stanford.edu

1 Introduction

The Soft X-ray Self-Seeding (SXRSS) infrastructure (or, at least room for it) will nominally be installed at the U8 girder location in the SXR undulator [1]. This location was chosen, in part, based on the expected electron beam quality coming from the beam delivery system (injector, accelerator and transport) [2]. Table 1 lists the nominal key electron beam parameters (slice) that are important for lasing as of the LCLS-II Final Design Report (FDR) [3]. However, results from global start-to-end optimizations using high-fidelity numerical

Table 1: Nominal electron beam parameters

Parameter	**Value**	**Unit**
Electron beam energy E_B	4.0	GeV
Electron beam current I_B	1.0	kA
Bunch charge Q	100	pC
Slice energy spread σ_E	0.5	MeV
Normalized emittance ε_N	0.45	μm
Average focusing β	15	m

particle simulations indicate that it is very difficult to compress the electron beam to a peak current $\geq$ 1.0 kA in the bunch core while maintaining the overall quality of the beam [4]. This technical note describes the impact the modified electron beam slice parameters at the entrance to the SXR undulator have on the predicted LCLS-II SXRSS performance. The conclusion reached from this study is that the infrastructure should be moved down two undulator girder locations from U8 to U10.

2 Start-to-end simulations

The start-to-end modeling and optimization of the LCLS-II free-electron laser from the cathode through the undulator using high fidelity numerical particle simulations is crucial for evaluating the expected FEL performance. These simulations have been performed for both the HXR and SXR undulators and for various charge distributions (20, 100, and 300 pC) across each of the undulator tuning ranges. Here, we focus on the 100 pC FEL performance in the SXR undulator, which shows the most promise of the three beam charges studied for SXRSS implementation [5].

2.1 Start-to-undulator simulations

Figure 1 shows the longitudinal phase space as well as the slice properties that are important for lasing of the 100 pC electron beam at the entrance to the SXR undulator. The current in the core of the electron beam is $\sim$ 800 Ampere while the slice energy spread is $\sim$ 520 keV

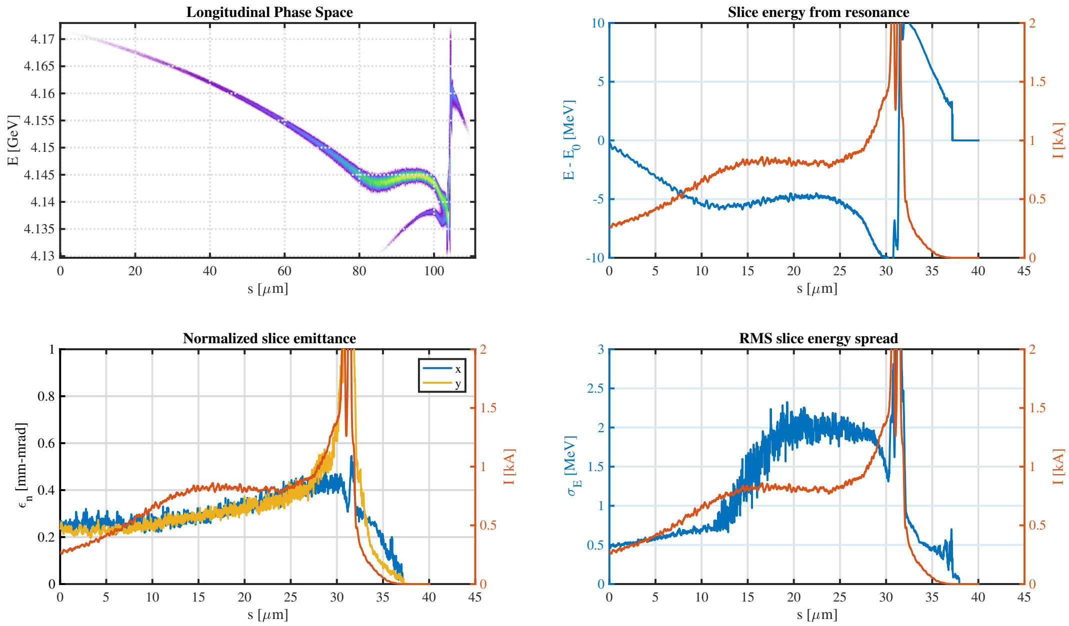

Figure 1: 100pC electron beam. Top left: Longitudinal phase space. The head of the beam is to the right. Top Right: Current (red) and slice energy deviation from resonant energy (blue) in the core. Bottom Left: Current (red) and transverse normalized slice emittance (x - blue, y - yellow) in the core. Bottom Right: Current (red) and RMS slice energy spread (blue) in the core.

and the normalized sliced emittance is ~ 0.35 mm-mrad in both transverse planes. While the SXR FEL performance is not so sensitive to the slice energy spread or, to some extent, the emittance, the peak current of the electron beam can have a sizeable impact on the available seed power.

2.2 FEL simulations

The FEL seed, after having undergone bandwidth narrowing in the SXRSS monochromator, needs to be significantly greater than the effective shot noise power in the beam for the seeded amplification to dominate any SASE contribution [6]. Typically, seeding $\sim 1.5 - 2$ orders of magnitude above the effective shot noise power allows the seeded radiation to saturate before any SASE components begin to significantly contaminate the spectrum. The effective shot noise power can be estimated using a relatively simple formula [7]:

$$P_{SN} \sim \frac{3\rho P_b}{N_c\sqrt{\pi \ln\left(N_c\right)}}. \tag{1}$$

Figure 2 shows the effective shot noise power, as calculated by equation 1, as a function of the resonant photon energy for the start-to-undulator 100 pC charge electron beam slice

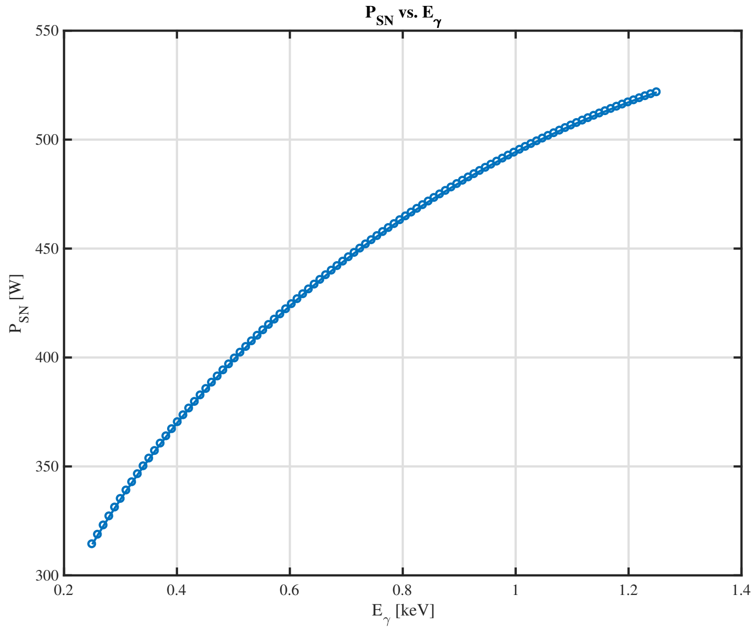

Figure 2: Effective shot noise power of the start-to-end 100 pC electron beam as a function of the resonant photon energy as given by equation 1.

parameters (in the core). The effective shot noise power lies between $\sim$ 300 W on the low end of the tuning range (E_{ph} = 250 eV) to $\sim$ 550 W on the high end of the tuning range (E_{ph} = 1.25 keV).

Figure 3 shows a typical SASE average power gain curve for the 100 pC electron beam using 8 SXR undulator sections. The radiation is tuned to be resonant at 1nm, which is at the high end of the tuning range. Here, the gain lengths are typically the longest and the effective shot noise power is the greatest making it the photon energy in the nominal undulator tuning range that is most difficult to satisfy the seed power requirements. The average radiation power after undulators 7 and 8 is $\sim$ 2 and $\sim$ 8 MW, respectively. The overall transmission of the SXRSS monochromator is roughly 3% for this photon energy range [8] while the bandwidth reduction factor is roughly a factor of 10, from 2.5 eV (2×10^{-3} is a typical SASE relative bandwidth after 8 undulators at this photon energy) to 0.25 eV (assuming a resolving power of R = 5000 in a Gaussian FWHM sense). Therefore, the total monochromator transmission efficiency reduces the incoming average SASE power to an effective seed power of 6 and 24 kW using 7 or 8 upstream SASE undulators, respectively. Using 8 SASE undulators provides a seed power that is roughly 50 times the effective shot noise power, which satisfies the seeding requirements, while using 7 SASE undulator sections clearly does not. Lower resonant photon energies nominally possess shorter gain lengths and lower effective shot noise powers. Therefore, using 8 SASE undulators to generate the seed should satisfy the seed power requirements across the LCLS-II SXRSS tuning range. However, an additional safety factor should be included to account for non-ideal optical coupling of the monochromatized radiation to the electron beam at the entrance of the

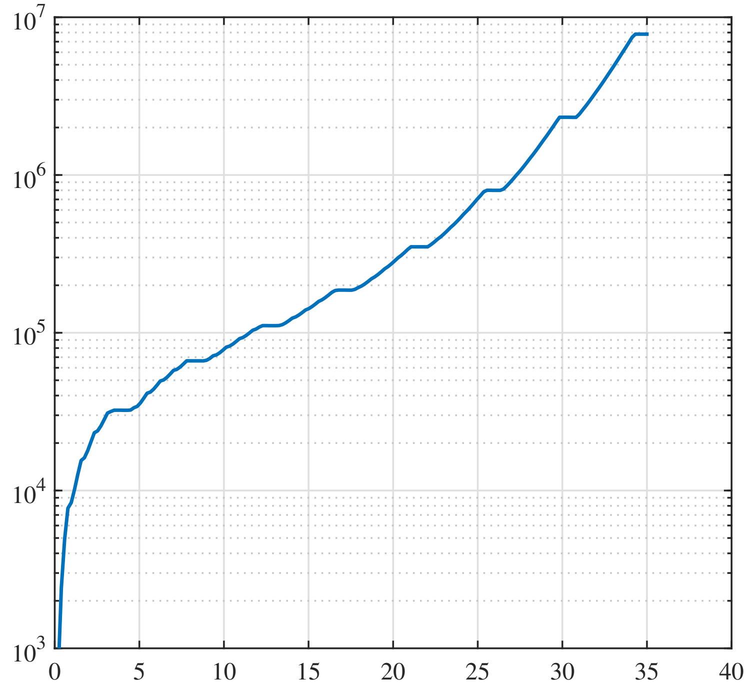

Figure 3: Average power SASE gain curve for the start-to-end 100 pC charge electron beam tuned to produce 1nm radiation in the LCLS-II SXR undulator.

seeded undulator as well as uncertainties regarding the quality of the electron beam coming from the injector. It is for these reasons that we propose moving the SXRSS infrastructure down two undulator girder locations to U10 from U8.

3 Impact on the movement of the SXRSS infrastructure on some advanced schemes

Moving the SXRSS infrastructure downstream two undulator girder locations will have an impact on various FEL schemes. A few of these schemes, as well as the consequences of moving the SXRSS location, are discussed below.

3.1 Tapering the SXRSS FEL

Moving the SXRSS infrastructure requires adding two undulators before the SXRSS infrastructure by removing two downstream undulators. Therefore, there will be two less undulators available for post-saturation tapering (12 rather than 14). Simulations indicate that the seeded FEL will saturate after roughly 11 undulators at the high end of the tuning range (E_{ph} = 1.25 keV). There is effectively no difference in post saturation power coming from an optimized taper of the seeded FEL if only 1 or 3 undulators contribute. Therefore, the seeded FEL performance is not sacrificed at the high end of the tuning range. The difference in output power at the low end of the tuning range will be negatively impacted by no more than a factor of 2, which is a very conservative estimate.

3.2 Two-color operation

Two-color operation, either by split-undulator, fresh-slice, or XLEAP generated schemes will be positively impacted by the infrastructure move. In these scenarios, the undulator is divided in two parts and are tuned to produce two different photon energies. A magnetic chicane in the middle of these undulator sections delays the electrons with respect to the X-rays, thus delaying the second X-ray pulse, and by extension the second X-ray photon energy, by the same amount. These schemes can operate across the entire tuning range of the SXR undulator. Ideally, the magnetic chicane would split the SXR undulator equally into two parts in order to balance the production of the two X-ray pulse energies equally and to ensure that saturation of each color can be reached. Moving the SXRSS infrastructure, including the magnetic chicane, from U8 to U10 helps to accomplish this task.

4 Conclusion

A careful study was performed using high-fidelity start-to-end numerical particle simulations to evaluate the impact on the SXRSS FEL performance in the LCLS-II SXR undulator. Moving the SXRSS infrastructure from U8 to U10 will ensure appropriate seed powers across the SXR undulator tuning range without significantly impacting the tapered performance. In addition, this infrastructure move will positively impact two-color FEL schemes by a more equitable distribution of undulators around the magnetic chicane.

References

[1] H.-D. Nuhn, "Undulator System", LCLS-II Physics Requirements Document LCLSII-3.2-PR-0038-R3 (2017).

[2] G. Marcus, "Soft X-ray Self-Seeding (SXRSS) System Requirements", LCLS-II Physics Requirements Document LCLSII-3.2-PR-0101-R0 (2014).

[3] LCLS-II Final Design Report, LCLSII-1.1-DR-0251-R0 (2015).

[4] G. Marcus, J. Qiang, "LCLS-II SCRF start-to-end simulations and global optimization as of September 2016," LCLS-II TN-17-04 (2017).

[5] E. Hemsing, et al., Soft X-ray FEL Seeding Studies for LCLS-II: Task Force Status Report, A White Paper by SLAC and LBNL (2017).

[6] J. Feldhaus et al., Opt. Comm., 140, 341 (1997).

[7] E.L. Saldin, E.A. Schneidmiller, M.V. Yurkov, "The Physics of Free Electron Lasers," Springer-Verlag, Berlin (1999).

[8] LCLS Soft X-ray Self-Seeding (SXRSS) System PRD, SLAC-I-081-101-003-00-R000 (2013).